HHS Public Access

Author manuscript

Cell Rep. Author manuscript; available in PMC 2016 January 08.

Published in final edited form as:

Cell Rep. 2015 December 29; 13(12): 2829–2841. doi:10.1016/j.celrep.2015.11.055.

Type I interferon transcriptional signature in neutrophils and high frequency of low-density granulocytes are associated with tissue damage in malaria

Bruno Coelho Rocha[1,2,3], **Pedro Elias Marques**[4], **Fabiana Maria de Souza Leoratti**[3], **Caroline Junqueira**[3], **Dhelio Batista Pereira**[5], **Lis Ribeiro do Valle Antonelli**[3], **Gustavo Batista Menezes**[4], **Douglas Taylor Golenbock**[#2], and **Ricardo Tostes Gazzinelli**[#1,2,3]

[1] Departamento de Bioquímica e Imunologia, ICB; Universidade Federal de Minas Gerais; Belo Horizonte, MG, 31270-901; Brazil.

[2] Department of Medicine; University of Massachusetts Medical School; Worcester, MA, 01605; United States of America.

[3] Centro de Pesquisas Rene Rachou, FIOCRUZ-MG; Belo Horizonte, MG, 30190-002; Brazil.

[4] Departamento de Morfologia, ICB; Universidade Federal de Minas Gerais; Belo Horizonte, MG, 31270-901; Brazil.

[5] Centro de Pesquisas em Medicina Tropical, FIOCRUZ-RO; Porto Velho, RO, 76812-329; Brazil.

[#] These authors contributed equally to this work.

SUMMARY

Neutrophils are the most abundant leukocyte population in the bloodstream, the primary compartment of *Plasmodium sp.* infection. Yet, the role of these polymorphonuclear cells in mediating either resistance or pathogenesis of malaria is poorly understood. We report that circulating neutrophils from malaria patients are highly activated, as indicated by a strong type I interferon transcriptional signature, increased expression of surface activation markers, the enhanced release of reactive oxygen species and myeloperoxidase, as well as the high frequency of low-density granulocytes. The activation of neutrophils was associated with increased levels of serum alanine and aspartate aminotransferases, indicating liver damage. In a rodent malaria model, we observed an intense recruitment of neutrophils to liver sinusoids. Neutrophil migration, IL-1β and chemokine expression as well as liver damage were all dependent on type I interferon

CONTACT INFORMATION, Ricardo T. Gazzinelli: ritoga@cpqrr.fiocruz.br; and Douglas T. Golenbock: douglas.golenbock@umassmed.edu..

AUTHOR CONTRIBUTIONS

Performed the experiments: B.C.R., P.E.M., F.M.S.L. and C.J.; Contributed with reagents, materials and analysis tools: R.T.G, D.T.G., G.B.M and L.R.V.A.; Coordinated the endemic area study: D.B.P.; Designed the experiments B.C.R., G.B.M., D.T.G. and R.T.G.; Wrote the manuscript: B.C.R., D.T.G. and R.T.G.

COMPETING FINANCIAL INTEREST

The authors declare no competing financial interest

signaling. The data suggests that type I interferon signaling have a central role in neutrophil activation and malaria pathogenesis.

INTRODUCTION

Malaria infected approximately 200 million people in 2013; an estimated 584,000 of these people died (World Health Organization, 2014). *Plasmodium vivax* is the most widespread human *Plasmodium* and represents a major social and economic health problem, especially in Latin America and Asia (Mueller et al., 2009; World Health Organization, 2014). On the other hand, *P. falciparum* is more prevalent in Africa and is responsible for most of the deaths from malaria (World Health Organization, 2014). Although the pathology associated with malaria occurs during the erythrocytic stage of infection, the liver is an important organ for malaria infection, as *Plasmodium* infects hepatocytes early in its life cycle, where it replicates asexually before reaching the blood stage (Prudêncio et al., 2006; Sturm et al., 2006). Furthermore, the liver is also an important organ for the trapping and clearance of *Plasmodium*-infected red blood cells (Krücken et al., 2009; Murthi et al., 2006). As a result, there is an intense recruitment of leukocytes to the liver during the acute phase of malaria (Haque et al., 2011).

The complexity of parasite-host interactions and the limited knowledge of the mechanisms by which *Plasmodium* trigger innate immune cells are the main impediments in understanding the pathogenesis of malaria (Gazzinelli et al., 2014). Surprisingly, the role of neutrophils in malaria has rarely been addressed.

Neutrophils are polymorphonuclear leukocytes (PMNs) capable of eliminating bacterial and fungal infections by multiple mechanisms (Mantovani et al., 2011). In addition to being the primary effectors of the immune response against microbial pathogens, neutrophils are also central mediators of inflammatory injury. However, the role of neutrophils in host resistance and pathogenesis of malaria is still controversial. Nevertheless, an altered function of neutrophils has been reported in both *P. vivax* and *P. falciparum* malaria (Cunnington et al., 2012; Leoratti et al., 2012).

Type I interferons (IFN) are cytokines that play an important role in the protection against viral infections. Type I interferons possess strong immunomodulatory activity. The production of type I IFNs has been associated with many other pathogens, including *Mycobacteria* (Antonelli et al., 2010), *Leishmania* (Xin et al., 2010) and *Plasmodium* (Aucan et al., 2003; Haque et al., 2014; Sharma et al., 2011). Type I IFNs modulate macrophages, monocytes, dendritic cells, and neutrophils through many different mechanisms (Salazar-Mather et al., 2002; Seo et al., 2011; Swiecki et al., 2011). Despite the high frequency of malaria, the roles of type I IFN in regulating neutrophils during infection have not been explored. Thus, we decided to focus on the importance of type I IFN in orchestrating neutrophil activation and function during malaria. We found that in both human and rodent malaria, neutrophil activation by type I IFN is associated with increased levels of circulating transaminases, indicative of liver pathology. Furthermore, we found that type I IFN modulates caspase-1/11 activation, pro-IL-1β and chemokine mRNA expression, as well as neutrophil migration to the liver of infected mice. Together, our results suggest

that type I IFNs are responsible for neutrophil-mediated liver pathology during both human and rodent malaria.

RESULTS

Neutrophils from *P. vivax* infected patients are highly activated

We observed an increase in the frequency and absolute number of neutrophils in the peripheral blood of *P. vivax*-infected patients (Figure 1A). To obtain these results, we used CD66b and CD15 as neutrophil markers. As shown in Figures S1A and S1B, over 98% of neutrophils from malaria patients expressed both markers. We also observed a low frequency of neutrophils containing hemozoin in blood smears of *P. vivax*-infected patients (Figure 1B, left panels). Arrows in central panels indicate parasites and hemozoin inside neutrophil vacuoles after 30 minutes of *in vitro* incubation with *P. vivax*-infected reticulocytes (PvRETs). Preparations of enriched PvRETs are shown in Figure 1B (right panels). To evaluate their activation status we assessed the kinetics of reactive oxygen species (ROS) production after stimulation with Phorbol 12-myristate 13-acetate (PMA) and with PvRETs. Total ROS production was evaluated in purified neutrophils by a luminol assay. Neutrophils from acutely infected patients produced significantly higher levels of ROS than neutrophils from healthy donors (HDs) when stimulated with PMA. These differences persisted over one hour of stimuli. Pre-treating cells with a NADPH oxidase inhibitor, diphenyleneiodonium chloride (DPI), completely abrogated ROS production in neutrophils from *P. vivax*-infected patients as well as in neutrophils from HDs. Similarly PvRETs also induced an augmented ROS production by neutrophils from *P. vivax*-infected patients (Figure 1C). We also measured myeloperoxidase (MPO) production by these cells after 24 hours of stimulation with PMA. Neutrophils from *P. vivax*-infected patients treated with PMA released significantly higher levels of MPO than neutrophils from the same patients after chemotherapy or neutrophils purified from HDs (Figure 1D). Altogether these results indicate that neutrophils are highly activated and become hyper-responsive during *P. vivax* infection.

P. vivax infection induces increased frequency of activated low-density granulocytes (LDGs) in the peripheral blood

Using conventional density gradient centrifugation to separate peripheral blood mononuclear cells (PBMCs) from malaria-infected patients, we found a higher frequency of a leukocyte subset with a high side scatter height (SSC-H) compared to those purified from healthy donors or cured patients (Figure 2A). We subsequently found that the frequency of $SSC^{hi}CD66b^{+}CD16^{+}$ cells within PBMCs was significantly higher in *P. vivax*-infected patients than uninfected controls (Figure 2B). These cells did not express CD14 nor MHC Class II molecules, confirming that they are not monocytes (Figure S3). Hence, this leukocyte subset, which also express CD15, was defined as LDGs (Brandau et al., 2011; Denny et al., 2010).

We next investigated the expression of activation markers within LDGs and neutrophils from 16 malaria patients, as well as neutrophils from HDs. We observed that the median fluorescence intensity (MFI) of CD15 and CD66b from LDGs of *P. vivax*-infected patients

was significantly higher than the MFI of these markers on purified neutrophils. There was no observable difference in either CD16 or CD11b expression in LDGs vs. PMNs (Figure 2C). CD34 and CD117, markers expressed on early progenitors, were not detected on either LDGs or neutrophils. Taken together, the profile of surface molecular expression suggests that the LDGs are activated neutrophils that have degranulated during *P. vivax* infection.

We next performed functional assays to determine the LDGs relevance in *P. vivax* infection. As LDGs express surface markers similar to granulocytic/neutrophilic myeloid derived suppressor cells (MDSC) (Brandau et al., 2011; Rodriguez et al., 2009), we tested their ability to inhibit T cell proliferation. We found that neither LDGs nor neutrophils from *P. vivax*-infected patients suppressed T cell proliferation after stimulation with αCD3/αCD28 (Figure 3A). Furthermore we showed that LDGs have an impaired migration towards CCL3 or IL-8, even though the expression of chemokines receptors was not reduced (Figure 3B). As we have previously shown, the migration to IL-8 was reduced in neutrophils from malaria patients (Leoratti et al., 2012). Interestingly, we observed that neutrophils from *P. vivax*-infected patients have an enhanced migration capacity to CCL3. This was associated with an increased expression of the chemokine receptor CCR5 (Figure 3B). Finally, we observed that LDGs have an increased phagocytic activity, similar to neutrophils from malaria patients, when compared to neutrophils from HDs (Figure 3C). Unexpectedly, we found low levels of phagocytosis of uninfected red blood cells (uRBCs) by LDGs as well as neutrophils from malaria patients and healthy donors. This background of our assay indicates low levels of internalization of CFSE-labeled uRBCs that may have been damaged during the experimental procedure. Nevertheless, the difference of phagocytosis between uRBCs and PvRETs is dramatic and indicates that infected reticulocytes are indeed actively internalized by neutrophils and LDGs from *P. vivax*-infected patients.

Neutrophils have an interferon transcriptional signature during *P. vivax* infection

We next profiled mRNA expression of highly enriched neutrophils (> 99% purity; see Figure S4A) collected from ten *P. vivax*-infected patients. We excluded the influence of significant monocyte contamination in these neutrophil preparations, as we could not detect $CD14^+$ cells in our preparation (Figure S4B). In addition, we analyzed our preparations for cytokines transcripts including *IFN-α* and *IFN-β* as well as chemokines that are produced by monocytes and not neutrophils, and they were not detected in this assay (Figure S4C). In agreement, different studies indicate that neutrophils do not produce type I IFN (Ohe et al., 2001; Yamaguchi et al., 1977). Furthermore, we assessed the mRNA and protein levels of IL-1β by neutrophils and monocytes from *P. vivax*-infected patients. Our results indicate that malaria infection does not induce an upregulation of neutrophils *IL-1β* transcripts and these cells did not produce IL-1β after LPS challenge (Figure S4D). A custom codeset for nanostring analysis was designed containing 98 genes related to inflammatory responses. Of 66 genes that were expressed by neutrophils, we found that 34 genes were differentially expressed upon *P. vivax* infection with a fold change greater than 1.8 and *p*-value lower than 0.05 compared to purified neutrophils from the same patients after chemotherapy (Table S1). From these 34 differentially expressed genes, 19 were considered to be IFN-stimulated genes (ISGs) (Figure 4A).

In order to get a clearer idea of what constitutes a "type I IFN signature", we purified neutrophils from HDs and stimulated them with either type I IFN or type II IFN (IFN-γ). We observed that most of the ISGs highly induced during malaria were predominantly type I IFN dependent, although IFN-γ also stimulated some of these genes, but generally to a lesser extent (Figure 4B). We also investigated ISG transcriptional expression in LDGs from *P. vivax*-infected patients. ISG expression by LDGs was lower than neutrophils, suggesting that these cell populations have different roles during malaria infection (Figure 4C). Finally, we observed a positive correlation between ISGs and AST serum levels in *P. vivax*-infected patients (Figure 4D). The malaria patients enrolled in this study had significantly increased levels of serum alanine (ALT) and aspartate (AST) aminotransferases, when compared to the same patients after therapy (Figure S4E). In summary, these data suggest that neutrophils from *P. vivax*-infected patients have a predominantly type I IFN transcriptional signature that positively correlates with liver damage.

Neutrophil recruitment and liver damage in *P. chabaudi* infected mice

Based on the hypothesis that neutrophils may be triggering liver damage during malaria, we investigated this phenomenon in mice infected with the blood stage of *P. chabaudi*. We first measured the recruitment of granulocytes at days 7, 11 and 14 post-infection by confocal intravital microscopy using anti-GR1 (Figure 5A). These results were confirmed by using the anti-Ly6G (clone 1A8) antibody that is more specific for neutrophils (Movie S1). The success of infection was confirmed by blood smears and by the presence of pigment (hemozoin) found only in infected livers (Figure 5A). We counted an average of 25.73 ± 4.69 (mean ± SEM) neutrophils per 10X field in non-infected mice (NI), whereas the mean of infected animals increased to 177.9 ± 22.93, 204.7 ± 11.44 and 140.9 ± 3.99 neutrophils per 10X field of view after 7, 11 and 14 days, respectively (Figure 5B). The serum ALT levels were measured in infected animals at different days and compared to the levels of NI mice. We noticed that mice after 7, 11 and 14 days of *P. chabaudi* infection had significantly higher levels of ALT than NI mice (Figure 5C). Because we observed the highest numbers of neutrophils as well as liver damage at day 11 after infection, we decided to use this time point for subsequent experiments.

To check if neutrophils were responsible for the observed liver damage during *P. chabaudi* infection, we depleted them by administering anti-Ly6G monoclonal antibody (clone 1A8) to infected and NI animals. Cells were subsequently assessed by flow cytometry. We detected an ~86% and ~76% reduction of the $CD11b^{+}Ly6C^{int}Ly6G^{+}$ cell population absolute numbers in peripheral blood and liver of infected mice treated with anti-Ly6G, respectively (Figure 5D and 5E). To confirm the specificity of neutrophil depletion, we analyzed the frequency and absolute cell number of other leukocytes in whole blood (Figure S5). We also assessed neutrophil depletion in the liver by confocal microscopy (Figure 5F). At d11 following infection, the mean neutrophil numbers per 10X field was 278.9 ± 17.6 (mean ± SEM) and 24.33 ± 4.1 in *P. chabaudi*-infected mice treated with the isotype control and anti-Ly6G, respectively. Uninfected animals showed similar neutrophils counts to infected mice treated with anti-Ly6G (isotype control: 12.9 ± 2.7; anti-Ly6G: 25.6 ± 4.2) (Figure 5G). Most importantly, serum ALT levels were reduced in *P. chabaudi*-infected mice treated with anti-Ly6G to a level that was almost that of uninfected controls (Figure

5H). Lastly, the neutrophil depletion resulted in a slight increase in parasitemia after 7 days of infection (Figure 5I). These data demonstrate that *P. chabaudi* infection directs neutrophil recruitment to the liver, which in turn induces tissue damage.

Type I IFN signaling drives neutrophil recruitment to the liver

Since we observed a predominantly type I IFN transcriptional signature in neutrophils from *P. vivax*-infected individuals, we used type I IFN receptor knockout mice (IFNαβR$^{-/-}$) to investigate the importance of type I IFN during malaria. Using confocal microscopy we observed a reduction of neutrophil recruitment in IFNαβR$^{-/-}$ mice after 11 days of infection (Figure 6A). Wild-type (WT) mice infected with *P. chabaudi* displayed a mean of 284.1 ± 13.4 (mean ± SEM) neutrophils per 10X FOV while the average count in IFNαβR$^{-/-}$ mice was 168.6 ± 9.7 neutrophils. As predicted, based on this reduction in the neutrophil recruitment, the ALT levels were significantly reduced in IFNαβR$^{-/-}$ mice to levels that were comparable to NI animals (Figure 6A).

To confirm that type I IFNs are inducing liver cells from *P. chabaudi* infected mice, we analyzed by qPCR the expression of ISGs in WT and IFNαβR$^{-/-}$ mice. We found that *IFI44*, *IRF7* and *IFIT1* were upregulated after *P. chabaudi* infection in WT mice but not induced in IFNαβR$^{-/-}$ mice (Figure 6B). We next decided to investigate whether the reduction in neutrophil recruitment in type I IFN receptor knockouts may be accounted for by a reduction in chemokines. Total mRNA was extracted from livers of NI and infected WT and IFNαβR$^{-/-}$ mice over the course of infection (days 3, 7 and 11). The loss of type I IFN signaling resulted in a marked decrease in the expression of *CCL3*, *CXCL1* and *IL-1β* mRNA after *P. chabaudi* infection (Figure 6C). Thus, our data suggest that type I IFN signaling triggers liver immunopathology during *P. chabaudi* infection by inducing the expression of chemokines and *IL-1β* involved in neutrophil recruitment.

Once we detected a modulation of *IL-1β* mRNA by type I IFN signaling, we used Caspase-1/11 knockout mice (Casp1/11$^{-/-}$) to study neutrophil recruitment to the liver. CD11b^{+}Ly6C^{int}Ly6G^{+} cells and serum ALT levels were significantly lower in *P. chabaudi*-infected Casp1/11$^{-/-}$ mice (Figure 6D and Figure S6), strongly suggesting a relationship between the relative neutropenia observed in the KO mice and the concomitant hepatitis as well as the conclusion that Caspase 1 and 11 are an important component of the liver damage.

DISCUSSION

The overt symptoms of malaria are due to the activation of innate immune cells and subsequent systemic inflammation. Indeed, when left untreated, malaria can be life-threatening. *P. falciparum* is responsible for most cases of severe malaria, while *P. vivax* is a relatively benign disease. However, despite its reputation for being a milder, *P. vivax* malaria is not only incapacitating but has been reported to occasionally cause severe illness with complications that include acute lung injury, respiratory distress, severe thrombocytopenia and severe anemia (Alexandre et al., 2010; Baird, 2013). Hepatic damage has also been described in both *P. falciparu*m and *P. vivax* malaria (Kochar et al., 2010;

Whitten et al., 2011), but the mechanisms of how malaria induces liver injury is poorly understood.

It is the common view that liver pathology during malaria infection is associated with hemolysis of infected red blood cells and the subsequent host inflammatory response to the products released from these infected cells. In animal models, elevated production of IFN-γ and IL-12 (Yoshimoto et al., 1998) and augmented infiltration of CD1d-unrestricted NKT cells were associated with liver injury (Adachi et al., 2004). The most commonly held view seems to be that malaria causes a brisk hemolysis, and that leukocyte recruitment to the liver subsequently results from immune activation due to the recognition of the products of erythrocytes. In turn, there is increased mRNA expression of adhesion molecules and chemokines in liver cells (Dey et al., 2012).

While our data concerning transaminasemia does not necessarily contradict this idea, our view is that the hepatic neutrophils are actually the cause, and not the result of hepatic injury. Indeed, in infectious disorders, neutrophils are typically the first cells to migrate to inflammatory sites where they fight invasive pathogens (Nathan, 2006). However, the activation of neutrophils, even when appropriate, may contribute to tissue damage during excessive inflammatory reactions (Marques et al., 2015b).

During the course of malaria, hepatitis and transaminasemia are extremely common but rarely considered to be clinically important, at least with respect to serious morbidity and mortality. Yet, given the systemic nature of malaria, it is likely that what can be seen on the surface of the liver by intravital microscopy is happening in other organs as well. Neutrophil-mediated injury to the vascular surface of post-capillary venules, the kidney and other sites of importance in life-threatening malaria might in fact result in an enhancement of the seriousness of infection. Unfortunately, like so many other aspects of innate immunity in malaria, there is only limited evidence to support this hypothesis. For example, early neutrophil depletion prevents the symptoms of cerebral malaria in mice by decreasing monocyte sequestration to the brain (Chen et al., 2000). However, this study used a monoclonal antibody (RB6-85) that also depletes dendritic cells and subpopulations of lymphocytes and monocytes (Daley et al., 2008), which makes interpretation of the results more complicated. Another tantalizing result was a report that *P. berghei* ANKA induces FcεRI expression in neutrophils and that activated neutrophil migrate to the brain and mediate the cerebral malaria (Porcherie et al., 2011).

An interesting observation that we have made is that *P. vivax* infections result in high circulating levels of activated low-density granulocytes, which is consistent with the hypothesis that neutrophils are activated during malaria. Low-density granulocytes have been reported in systemic lupus erythematosus (SLE) (Denny et al., 2010), HIV (Cloke et al., 2012), psoriasis (Lin et al., 2011) and in certain types of cancer patients (Brandau et al., 2011; Rodriguez et al., 2009). The origin and activation status of LDGs are controversial due to differences found in nuclear morphology and the expression of surface markers (Brandau et al., 2011; Denny et al., 2010). Our results indicate that LDGs are mature cells based on their surface activation marker expression, as they do not express markers of neutrophil progenitors. Although the LDGs from *P. vivax*-infected patients resemble the

granulocytic/neutrophilic MDSCs in terms of surface markers expression, they did not inhibit T cells proliferation (Brandau et al., 2011; Rodriguez et al., 2009). Hence, we propose that LDGs from *P. vivax*-infected patients are highly activated degranulated neutrophils, and are major contributors to systemic inflammation.

We have previously reported that PBMC have a type I IFN signature in patients with uncomplicated *P. falciparum* malaria (Sharma et al., 2011). This report expands upon that observation as we have demonstrated a similar interferon signature in neutrophils during malaria. A similar pattern of gene expression has been reported in PMNs from active tuberculosis patients and correlates with disease severity, supporting a role of type I IFN in TB pathogenesis (Berry et al., 2010). The observation that ISGs expression in neutrophils correlates with hepatic damage in *P. vivax* malaria patients suggests that neutrophils are migrating to the liver. Consistently, we found an enhanced expression of CCR5 and migration towards a CCL3 gradient in activated neutrophils from *P. vivax* patients.

Importantly, a high frequency of hemozoin containing neutrophils are seen in the circulation of patients with high parasitemia and severe disease (Lyke et al., 2003). Indeed, our results suggest that neutrophils may be also contributing to control parasitemia in *P. vivax* infected patients. Thus, we observed an augmented phagocytosis of PvRET and ROS production by neutrophils from *P. vivax* patients. These results are consistent with a study showing that neutrophils from periodontitis patients displayed an ISG signature, which is associated with enhanced ROS production (Wright et al., 2008). In agreement with our results demonstrating that neutrophil depletion results in a small increase in parasitemia of mice infected with *P. chabaudi*, these studies suggest that neutrophils may play a role in resistance to human malaria.

We then decided to investigate the role of type I IFN signaling and neutrophils in a malaria experimental model. We found that type I IFN promotes neutrophils migration to the liver in *P. chabaudi*-infected mice. Consistent with this, previous reports have demonstrated that type I IFN signaling promotes leukocytes recruitment to the liver during the pre-erythrocytic stage of malaria (Liehl et al., 2014; Miller et al., 2014).

Furthermore we found that caspase-1/11 was also necessary to mediate neutrophils recruitment to the liver. Malarial hemozoin (Hz), has been shown to activate the NLRP3 and absent in melanoma (AIM2) inflammasome and to trigger IL-1β production (Kalantari et al., 2014; Shio et al., 2009). In addition, Hz also induces mRNA expression of several chemokines such as *CCL3*, *CCL4* and *CXCL2* in the liver (Jaramillo et al., 2004). Taking in consideration our own results and those published elsewhere, we propose that type I IFN promotes the expression of caspase-1/11 in the liver, which will generate active IL-1β, a potent inducer of chemokines that effectively recruit neutrophils.

In conclusion, our results show a pronounced expression of activation markers, transcriptional signature of ISGs, increased phagocytic activity, enhanced release of reactive oxygen species and myeloperoxidase, and high circulating levels of LDGs during *P. vivax* malaria. While there is a recent literature suggesting “innate immunity memory” or “trained immunity”, this interpretation implies that this stage of augmented response to microbial

stimuli is long lasting (Quintin et al., 2014). As neutrophils are short-lived cells, and the observed effect comes to baseline (similar to HDs) after treatment, we favor the hypothesis of neutrophil priming rather than “innate immunity memory” or “trained immunity”. Importantly, our results indicate a potential pathophysiological role for neutrophils in liver damage during malaria. Therefore there is a need to look more closely at the role of neutrophils in the multi organ dysfunction that accompanies truly severe disease.

EXPERIMENTAL PROCEDURES

Patients

This study was reviewed and approved by the Ethical Committees on Human Experimentation from Centro de Pesquisas em Medicina Tropical (CEPCEPEM 096/2009), the Brazilian National Ethical Committee (CONEP 15653) from Ministry of Health and by the Institutional Review Board from the University of Massachusetts Medical School (IRB-ID11116_1). Patients with acute uncomplicated *P. vivax* malaria (n=44) were enrolled based on their symptoms of fever and/or rigors in the last 24 hours before recruitment in the outpatient malaria clinic in Porto Velho (Table S2). Written informed consent was obtained before enrollment of all subjects. Up to 100 mL of peripheral blood was collected immediately after confirmation of *P. vivax* infection by a standard thick blood smear and 30–45 days after chemotherapy. Patients were treated with chloroquine and primaquine according to the Brazilian Ministry of Health and all patients included in this study were parasitologically cured after treatment. Peripheral blood was also collected from healthy donors living in an endemic area and negative for *P. vivax* infection.

Purification of neutrophils and low-density granulocytes and flow cytometry analysis

Neutrophils from *P. vivax*-infected patients before and after treatment and from HDs were isolated by Ficoll-Hypaque (GE Biosciences) gradient followed by a Human Neutrophil Enrichment Kit (STEMCELL Technologies) according to the manufacturer's instructions. Neutrophil purity was assessed by flow cytometry staining with specific monoclonal antibodies listed in Table S3. LDGs were purified from PBMCs of *P. vivax*-infected patients by the CD66abce microbead kit (Miltenyi Biotec). LDGs were also analyzed by flow cytometry within PBMCs using forward (FSC-H) and side scatter height (SSC-H) and specific mAbs (Table S3). Stained cells were acquired using a FACSCan upgraded with a second laser (5 colors) with Cellquest Pro and Rainbow from Cytek (BD). Data analysis was carried out using FlowJo Version 9.4.10.

Phagocytosis and enrichment of *P. vivax*-infected reticulocytes (PvRETs)

Enrichment of PvRETs were performed using a 45% Percoll gradient as described previously (Carvalho et al., 2010). Non-infected red blood cells (uRBC) were used as a negative control in the phagocytosis assay. The purity of PvRETs was determined by optic microscopy. Purified PvRETs and uRBCs were stained with 1 μM carboxyfluorescein succinimidyl ester (CFSE). Purified neutrophils and LDGs from *P. vivax*-infected patients were incubated for one hour at 37°C, 5% CO_2 with purified PvRETs or uRBCs previously labeled with CFSE (neutrophils or LDGs:PvRETs or uRBCs ratio, 2:1). The frequencies of neutrophils and LDGs positive for CFSE were determined by flow cytometry.

Chemotaxis assay

Seventy five thousand purified neutrophils and LDGs from *P. vivax*-infected patients and neutrophils from HD were allowed to migrate through a 5 μm pore 96-well microchamber (NeuroProbe, Gaithersburg, MD) toward CCL3 (50 ng/ml), IL-8 (CXCL8) (10 ng/ml), or medium alone. Migrated cells were counted under a light microscope.

T cell proliferation assay

PBMCs from *P. vivax*-infected patients after depletion of LDGs were harvested and stained with 1μM CFSE (Invitrogen). These cells were stimulated with soluble αCD3 (1 μg/mL) and αCD28 (0.5 μg/mL) in the presence or absence of LDGs or neutrophils (PBMC:LDGs or neutrophils ratio, 2:1). After four days of coculture, CFSE fluorescence intensity was analyzed by FlowJo Version 9.4.10. T cell proliferation was determined after gating the $CD3^+$ population and measuring the percentage of $CFSE^{low}$ T cells.

Nanostring analysis

Purified human neutrophils and LDGs were lysed in RLT buffer (Qiagen) supplemented with β-mercaptoethanol and used to determine mRNA abundance by Nanostring Technology (Geiss et al., 2008). In brief, lysates were hybridized with the capture and reporter probes overnight at 65°C. Then, they were loaded onto the nCounter prep station and quantified with the nCounter Digital Analyzer. For side-by-side comparisons of nCounter experiments, data was normalized with internal positive controls and with 7 housekeeping genes. Finally, data from *P. vivax*-infected cells were normalized to the same cells 30-45 days after treatment. Differences in gene expression between the 2 conditions were considered significant if $p < 0.05$ as defined by multiple T test followed by false discovery rate approach and if the fold change was greater than 1.8. The heatmap was constructed using $\log_2$ transformed data and the Tiger Multi Experiment Viewer software version 4.8.

ROS detection and MPO quantification

For luminol-based ROS measurements, 5×10^5 neutrophils from *P. vivax*-infected patients or HDs were plated in clear-bottom 96-well plates (Corning) in triplicate. Cells were stimulated with 100 ng/mL PMA, 2.5×10^5 PvRET or left untreated with medium for 2 hours in the presence of 100 μM luminol. Where indicated, the ROS production inhibitor, diphenyleneiodonium (DPI) 5 μM was added to cell culture 30 minutes before stimuli. Chemiluminescence kinetics was measured by Synergy HT (Biotek) microplate reader.

One million purified neutrophils from *P. vivax*–infected individuals before and after treatment were stimulated with 100 ng/mL of PMA or left untreated for 24 hours. Supernatants were collected and MPO levels were measured by an MPO Elisa Kit (Calbiochem) according to the manufacturer's instructions.

Mice, parasites and infection

C57BL/6, 129 Svev, $IFN\alpha\beta R^{-/-}$ and $Casp1/11^{-/-}$ mice (8-12 weeks) were bred and maintained under specific pathogen-free conditions in accordance with the Institutional Animal Care and Use Committee (IACUC). All protocols developed for this work were

approved by the IACUC at the University of Massachusetts Medical School (ID-1369-11) and by the Council of Animal Experimentation of Oswaldo Cruz Foundation (CEUA protocol 61/13-2).

The *Plasmodium chabaudi chabaudi* AS strain was used for experimental infections. This strain was maintained in C57BL/6 mice by intraperitoneal injection of 1×10^5 infected erythrocytes (iRBCs) once a week. Parasitemia was checked every three days.

Quantification of liver neutrophils

Mouse primary nonparenchymal cells were purified from *P. chabaudi*-infected and NI mice using a 35% Percoll gradient followed by red blood cells lysis, as described before (Liehl et al., 2014). Viable nonparenchymal cells were counted by trypan blue exclusion and stained with specific mAbs (Table S3) to determine the frequency of neutrophils among liver leukocytes by flow cytometry. Stained cells were acquired using a LSRII flow cytometer (BD). Data analysis was carried out using FlowJo Version 9.4.10.

P. chabaudi-infected and NI mice were also used for confocal intravital microscopy neutrophil quantification, as described previously (Marques et al., 2015a). PE-conjugated anti-GR1 (4μg/mouse; 40μg/ml, eBioscience) was injected i.v. 10 minutes before imaging. Images were obtained using a C2 Eclipse Ti confocal microscope. Neutrophil counts were performed using Image J software.

Neutrophil depletion and ALT measurement

In vivo neutrophil depletion was performed by administering four i.p. injections of anti-Ly6G antibody (500μg/dose, clone 1A8; BioXCell) or an isotype control (500μg/dose, clone 2A3; BioXCell): 1 day before *P. chabaudi* infection, and 2, 6 and 10 days after infection. Serum alanine aminotransferase (ALT) activity was performed using a kinetic test (Bioclin).

qRT-PCR Analysis

Total RNA from livers of non-infected (Control), 3 day-, 7 day- or 11 day-infected mice were isolated by TRIzol Reagent (Invitrogen). Quantitative PCR was carried out with Platinum SYBR Green protocol (Invitrogen) on an Applied Biosystems 7500 Real Time PCR System using primers listed in Table S4. Relative quantification was performed using standard curve analysis and the expression data were presented as mean of normalized expression to the *GAPDH* level of three biological replications.

Statistical analysis

Statistical analysis was performed using GraphPad Prism 6 software. The results were analyzed using two-tailed paired t-test and One-way ANOVA between the groups. Mann-Whitney (MW) test was used when data did not fit a Gaussian distribution. Data shown are representative of at least two independent experiments. Differences were considered to be statistically significant when $P \leq 0.05$.

Supplementary Material

Refer to Web version on PubMed Central for supplementary material.

ACKNOWLEDGMENTS

We are grateful to Melanie Trombly for critically reviewing this manuscript, to the Program for Technological Development in Tools for Health–PDTIS- FIOCRUZ for use of its facilities, to Dr. Luiz Hildebrando Pereira da Silva for providing the logistics for development of this work in the endemic area of Porto Velho, and to the clinic, laboratory and administrative staff, field workers and subjects who participated in the study. Supported by the National Institute of Health (AI079293), National Institute of Science and Technology for Vaccines, Conselho Nacional de Desenvolvimento Científico e Tecnológico (CNPq) and Coordenação de Aperfeiçoamento de Pessoal de Ensino Superior (CAPES).

REFERENCES

Adachi K, Tsutsui H, Seki E, Nakano H, Takeda K, Okumura K, Van Kaer L, Nakanishi K. Contribution of CD1d-unrestricted hepatic DX5+ NKT cells to liver injury in Plasmodium berghei-parasitized erythrocyte-injected mice. Int. Immunol. 2004; 16:787–798. [PubMed: 15096477]

Alexandre MA, Ferreira CO, Siqueira AM, Magalhães BL, Mourão MPG, Lacerda MV, Alecrim MDGC. Severe Plasmodium vivax malaria, Brazilian Amazon. Emerging Infect. Dis. 2010; 16:1611–1614. [PubMed: 20875292]

Antonelli LRV, Gigliotti Rothfuchs A, Goncalves R, Roffê E, Cheever AW, Bafica A, Salazar AM, Feng CG, Sher A. Intranasal Poly-IC treatment exacerbates tuberculosis in mice through the pulmonary recruitment of a pathogen-permissive monocyte/macrophage population. J. Clin. Invest. 2010; 120:1674–1682. [PubMed: 20389020]

Aucan CC, Walley AJA, Hennig BJWB, Fitness JJ, Frodsham AA, Zhang LL, Kwiatkowski DD, Hill AVSA. Interferon-alpha receptor-1 (IFNAR1) variants are associated with protection against cerebral malaria in the Gambia. Genes Immun. 2003; 4:275–282. [PubMed: 12761564]

Baird JK. Evidence and implications of mortality associated with acute Plasmodium vivax malaria. Clin. Microbiol. Rev. 2013; 26:36–57. [PubMed: 23297258]

Berry MPR, Graham CM, McNab FW, Xu Z, Bloch SAA, Oni T, Wilkinson KA, Banchereau R, Skinner J, Wilkinson RJ, et al. An interferon-inducible neutrophil-driven blood transcriptional signature in human tuberculosis. Nature. 2010; 466:973–977. [PubMed: 20725040]

Brandau S, Trellakis S, Bruderek K, Schmaltz D, Steller G, Elian M, Suttmann H, Schenck M, Welling J, Zabel P, et al. Myeloid-derived suppressor cells in the peripheral blood of cancer patients contain a subset of immature neutrophils with impaired migratory properties. J. Leukoc. Biol. 2011; 89:311–317. [PubMed: 21106641]

Carvalho BO, Lopes SCP, Nogueira PA, Orlandi PP, Bargieri DY, Blanco YC, Mamoni R, Leite JA, Rodrigues MM, Soares IS, et al. On the cytoadhesion of Plasmodium vivax-infected erythrocytes. J. Inf. Dis. 2010; 202:638–647. [PubMed: 20617923]

Chen L, Zhang Z, Sendo F. Neutrophils play a critical role in the pathogenesis of experimental cerebral malaria. Clin. Exp. Immunol. 2000; 120:125–133. [PubMed: 10759773]

Cloke T, Munder M, Taylor G, Müller I, Kropf P. Characterization of a novel population of low-density granulocytes associated with disease severity in HIV-1 infection. PLoS ONE. 2012; 7:e48939. [PubMed: 23152825]

Cunnington AJ, Njie M, Correa S, Takem EN, Riley EM, Walther M. Prolonged neutrophil dysfunction after Plasmodium falciparum malaria is related to hemolysis and heme oxygenase-1 induction. J. Immunol. 2012; 189:5336–5346. [PubMed: 23100518]

Daley JM, Thomay AA, Connolly MD, Reichner JS, Albina JE. Use of Ly6G-specific monoclonal antibody to deplete neutrophils in mice. J. Leukoc. Biol. 2008; 83:64–70. [PubMed: 17884993]

Denny MF, Yalavarthi S, Zhao W, Thacker SG, Anderson M, Sandy AR, McCune WJ, Kaplan MJ. A Distinct Subset of Proinflammatory Neutrophils Isolated from Patients with Systemic Lupus Erythematosus Induces Vascular Damage and Synthesizes Type I IFNs. J. Immunol. 2010; 184:3284–3297. [PubMed: 20164424]

Dey S, Bindu S, Goyal M, Pal C, Alam A, Iqbal MS, Kumar R, Sarkar S, Bandyopadhyay U. Impact of Intravascular Hemolysis in Malaria on Liver Dysfunction: Involvement Of Hepatic Free Heme Overload, Nf-kB Activation, And Neutrophil Infiltration. J. Biol. Chem. 2012; 287:26630–26646. [PubMed: 22696214]

Gazzinelli RT, Kalantari P, Fitzgerald KA, Golenbock DT. Innate sensing of malaria parasites. Nat. Rev. Immunol. 2014; 14:744–757. [PubMed: 25324127]

Geiss GKG, Bumgarner RER, Birditt BB, Dahl TT, Dowidar NN, Dunaway DLD, Fell HPH, Ferree SS, George RDR, Grogan TT, et al. Direct multiplexed measurement of gene expression with color-coded probe pairs. Nat. Biotechnol. 2008; 26:317–325. [PubMed: 18278033]

Haque A, Best SE, Amante FH, Ammerdorffer A, de Labastida F, Pereira T, Ramm GA, Engwerda CR. High parasite burdens cause liver damage in mice following Plasmodium berghei ANKA infection independently of CD8(+) T cell-mediated immune pathology. Infect. Immun. 2011; 79:1882–1888. [PubMed: 21343349]

Haque A, Best SE, de Oca MM, James KR, Ammerdorffer A, Edwards CL, de Labastida Rivera F, Amante FH, Bunn PT, Sheel M, et al. Type I IFN signaling in CD8-DCs impairs Th1-dependent malaria immunity. J. Clin. Invest. 2014; 124:2483–2496. [PubMed: 24789914]

Jaramillo M, Plante I, Ouellet N, Vandal K, Tessier PA, Olivier M. Hemozoin-inducible proinflammatory events in vivo: potential role in malaria infection. J. Immunol. 2004; 172:3101–3110. [PubMed: 14978116]

Kalantari P, DeOliveira RB, Chan J, Corbett Y, Rathinam V, Stutz A, Latz E, Gazzinelli RT, Golenbock DT, Fitzgerald KA. Dual engagement of the NLRP3 and AIM2 inflammasomes by plasmodium-derived hemozoin and DNA during malaria. Cell Rep. 2014; 6:196–210. [PubMed: 24388751]

Kochar DK, Tanwar GS, Khatri PC, Kochar SK, Sengar GS, Gupta A, Kochar A, Middha S, Acharya J, Saxena V, et al. Clinical features of children hospitalized with malaria--a study from Bikaner, northwest India. Am. J. Trop. Med. Hyg. 2010; 83:981–989. [PubMed: 21036824]

Krücken J, Delić D, Pauen H, Wojtalla A, El-Khadragy M, Dkhil MA, Mossmann H, Wunderlich F. Augmented particle trapping and attenuated inflammation in the liver by protective vaccination against Plasmodium chabaudi malaria. Malar. J. 2009; 8:54–54. [PubMed: 19341445]

Leoratti, F.M. de S.; Trevelin, SC.; Cunha, FQ.; Rocha, BC.; Costa, PAC.; Gravina, HD.; Tada, MS.; Pereira, DB.; Golenbock, DT.; do Valle Antonelli, LR., et al. Neutrophil Paralysis in Plasmodium vivax Malaria. PLoS Negl. Trop. Dis. 2012; 6:e1710. [PubMed: 22745844]

Liehl P, Zuzarte-Luís V, Chan J, Zillinger T, Baptista F, Carapau D, Konert M, Hanson KK, Carret C, Lassnig C, et al. Host-cell sensors for Plasmodium activate innate immunity against liver-stage infection. Nat. Med. 2014; 20:47–53. [PubMed: 24362933]

Lin AM, Rubin CJ, Khandpur R, Wang JY, Riblett M, Yalavarthi S, Villanueva EC, Shah P, Kaplan MJ, Bruce AT. Mast cells and neutrophils release IL-17 through extracellular trap formation in psoriasis. J. Immunol. 2011; 187:490–500. [PubMed: 21606249]

Lyke KE, Diallo DA, Dicko A, Kone A, Coulibaly D, Guindo A, Cissoko Y, Sangare L, Coulibaly S, Dakouo B, et al. Association of intraleukocytic Plasmodium falciparum malaria pigment with disease severity, clinical manifestations, and prognosis in severe malaria. Am. J. Trop. Med. Hyg. 2003; 69:253–259. [PubMed: 14628940]

Mantovani A, Cassatella MA, Costantini C, Jaillon S. Neutrophils in the activation and regulation of innate and adaptive immunity. Nat. Rev. Immunol. 2011; 11:519–531. [PubMed: 21785456]

Marques PE, Antunes MM, David BA, Pereira RV, Teixeira MM, Menezes GB. Imaging liver biology in vivo using conventional confocal microscopy. Nat. Protoc. 2015a; 10:258–268. [PubMed: 25569332]

Marques PE, Oliveira AG, Pereira RV, David BA, Gomides LF, Saraiva AM, Pires DA, Novaes JT, Patricio DO, Cisalpino D, et al. Hepatic DNA deposition drives drug-induced liver injury and inflammation in mice. Hepatology. 2015b; 61:348–360. [PubMed: 24824608]

Miller JL, Sack BK, Baldwin M, Vaughan AM, Kappe SHI. Interferon-mediated innate immune responses against malaria parasite liver stages. Cell Rep. 2014; 7:436–447. [PubMed: 24703850]

Mueller I, Galinski MR, Baird JK, Carlton JM, Kochar DK, Alonso PL, del Portillo HA. Key gaps in the knowledge of Plasmodium vivax, a neglected human malaria parasite. Lancet Infect. Dis. 2009; 9:555–566. [PubMed: 19695492]

Murthi P, Kalionis B, Ghabrial H, Dunlop ME, Smallwood RA, Sewell RB. Kupffer cell function during the erythocytic stage of malaria. J. Gastroenterol. Hepatol. 2006; 21:313–318. [PubMed: 16460493]

Nathan C. Neutrophils and immunity: challenges and opportunities. Nat. Rev. Immunol. 2006; 6:173–182. [PubMed: 16498448]

Ohe, von der M, Altstaedt J, Gross U, Rink L. Human neutrophils produce macrophage inhibitory protein-1beta but not type i interferons in response to viral stimulation. J. Interf. Cytok. Res. 2001; 21:241–247.

Porcherie A, Mathieu C, Peronet R, Schneider E, Claver J, Commere PH, Kiefer-Biasizzo H, Karasuyama H, Milon G, Dy M, et al. Critical role of the neutrophil-associated high-affinity receptor for IgE in the pathogenesis of experimental cerebral malaria. J. Exp. Med. 2011; 208:2225–2236. [PubMed: 21967768]

Prudêncio M, Rodriguez A, Mota MM. The silent path to thousands of merozoites: the Plasmodium liver stage. Nat. Rev. Microbiol. 2006; 4:849–856. [PubMed: 17041632]

Quintin J, Cheng S-C, van der Meer JWM, Netea MG. Innate immune memory: towards a better understanding of host defense mechanisms. Curr. Opin. Immunol. 2014; 29:1–7. [PubMed: 24637148]

Rodriguez PC, Ernstoff MS, Hernandez C, Atkins M, Zabaleta J, Sierra R, Ochoa AC. Arginase I-producing myeloid-derived suppressor cells in renal cell carcinoma are a subpopulation of activated granulocytes. Cancer Res. 2009; 69:1553–1560. [PubMed: 19201693]

Salazar-Mather TP, Lewis CA, Biron CA. Type I interferons regulate inflammatory cell trafficking and macrophage inflammatory protein 1alpha delivery to the liver. J. Clin. Invest. 2002; 110:321–330. [PubMed: 12163451]

Seo S-U, Kwon H-J, Ko H-J, Byun Y-H, Seong BL, Uematsu S, Akira S, Kweon M-N. Type I Interferon Signaling Regulates Ly6Chi Monocytes and Neutrophils during Acute Viral Pneumonia in Mice. PLoS Pathog. 2011; 7:e1001304. [PubMed: 21383977]

Sharma S, DeOliveira RB, Kalantari P, Parroche P, Goutagny N, Jiang Z, Chan J, Bartholomeu DC, Lauw F, Hall JP, et al. Innate immune recognition of an AT-rich stem-loop DNA motif in the Plasmodium falciparum genome. Immunity. 2011; 35:194–207. [PubMed: 21820332]

Shio MT, Tiemi Shio M, Eisenbarth SC, Savaria M, Vinet AF, Bellemare M-J, Harder KW, Sutterwala FS, Bohle DS, Descoteaux A, et al. Malarial hemozoin activates the NLRP3 inflammasome through Lyn and Syk kinases. PLoS Pathog. 2009; 5:e1000559. [PubMed: 19696895]

Sturm A, Amino R, van de Sand C, Regen T, Retzlaff S, Rennenberg A, Krueger A, Pollok J-M, Menard R, Heussler VT. Manipulation of host hepatocytes by the malaria parasite for delivery into liver sinusoids. Science. 2006; 313:1287–1290. [PubMed: 16888102]

Swiecki M, Wang Y, Vermi W, Gilfillan S, Schreiber RD, Colonna M. Type I interferon negatively controls plasmacytoid dendritic cell numbers in vivo. J. Exp. Med. 2011; 208:2367–2374. [PubMed: 22084408]

Whitten R, Milner DA, Yeh MM, Kamiza S, Molyneux ME, Taylor TE. Liver pathology in Malawian children with fatal encephalopathy. Hum. Pathol. 2011; 42:1230–1239. [PubMed: 21396681]

World Health Organization. World Malaria Report 2014. 2014

Wright HJ, Matthews JB, Chapple ILC, Ling-Mountford N, Cooper PR. Periodontitis associates with a type 1 IFN signature in peripheral blood neutrophils. J. Immunol. 2008; 181:5775–5784. [PubMed: 18832737]

Xin L, Vargas-Inchaustegui DA, Raimer SS, Kelly BC, Hu J, Zhu L, Sun J, Soong L. Type I IFN receptor regulates neutrophil functions and innate immunity to Leishmania parasites. J. Immunol. 2010; 184:7047–7056. [PubMed: 20483775]

Yamaguchi T, Handa K, Shimizu Y, Abo T, Kumagai K. Target cells for interferon production in human leukocytes stimulated by sendai virus. J. Immunol. 1977; 118:1931–1935. [PubMed: 193987]

Yoshimoto T, Takahama Y, Wang CR, Yoneto T, Waki S, Nariuchi H. A pathogenic role of IL-12 in blood-stage murine malaria lethal strain Plasmodium berghei NK65 infection. J. Immunol. 1998; 160:5500–5505. [PubMed: 9605153]

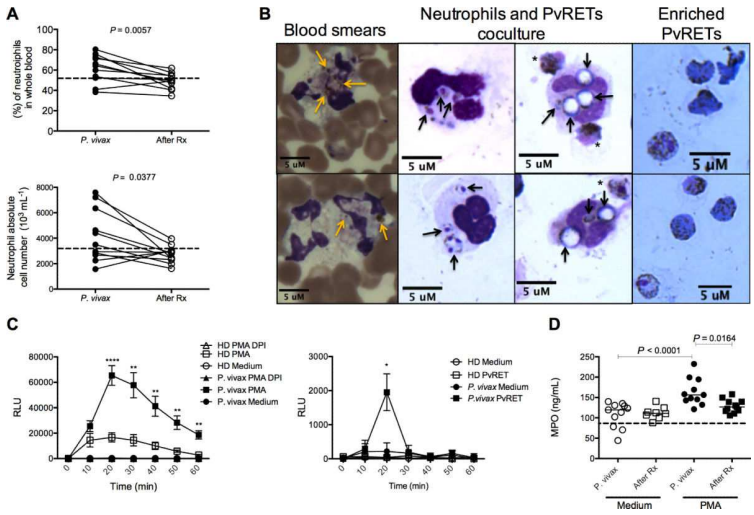

Figure 1. Neutrophils from *P. vivax*-infected patients display a highly activated phenotype

(A) Frequency (top panel) and absolute numbers (bottom panel) of neutrophils stained within whole blood from *P. vivax*-infected patients before and 30-45 days after treatment (After Rx). Each pair of circle connected by a line represents a single patient (n=11). The absolute numbers were calculated based on their frequency and total leukocytes numbers. (B) Left panels: neutrophils containing hemozoin (yellow arrows) from *P. vivax*-infected patients blood smears. Central panels: parasite components and hemozoin in vacuoles (black arrows) of neutrophils after *in vitro* incubation with PvRETs (*). Right panels: enriched PvRETs from peripheral blood of malaria patients by Percoll gradient. Scale bars: 5 μM. (C) The kinetics of ROS production by neutrophils from patients with acute *P. vivax* infections or healthy donors (HDs) cultured in medium alone or with 100 ng/ml Phorbol 12-myristate 13-acetate (PMA) in the presence or absence of ROS inhibitor, DPI (5 μM) (n=5-7) (left panel) or stimulated with purified *P. vivax*-infected reticulocytes (PvRET) (neutrophils:PvRET ratio, 2:1) (n=4) (right panel). Luminol was measured by chemiluminescence (RLU) for 60 minutes. Data are represented as mean ± SEM. The differences are relative to the HDs. *0.05>P>0.01; **0.01>P>0.001; ****P<0.0001. Individual values of PMA- or PvRET-induced ROS released by neutrophils from *P. vivax*-infected patients and HDs are depicted in Figure S2. (D) Myeloperoxidase (MPO) levels in supernatants of unstimulated and PMA (100 ng/mL) activated neutrophils from *P. vivax*-infected patients before and after treatment (After Rx) for 24 hours (n=11). (A and D) Dashed lines represent the median of given measurements for 5 healthy donors. See also Figures S1 and S2.

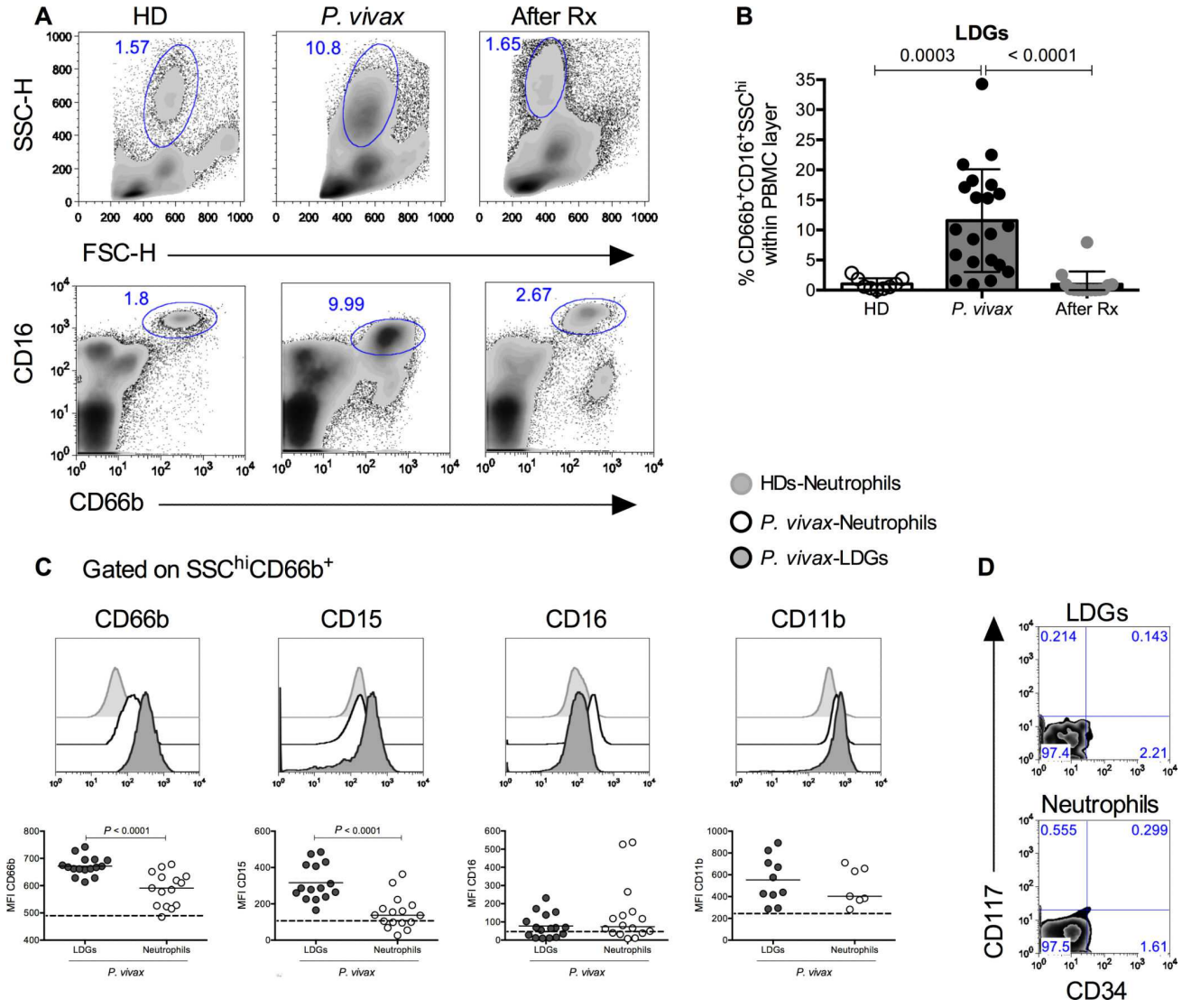

Figure 2. Low-density granulocytes are increased and activated in PBMCs from patients with acute *P. vivax*-infections

(A) Representative density plots and (B) bar graph indicating the frequencies of $SSC^{hi}CD66b^{+}CD16^{+}$ (LDGs) within PBMCs of HDs (white circles) (n=9), *P. vivax*-infected patients before (black circles) (n=21) and after treatment (After Rx) (gray circles) (n=14). Data are represented as mean ± SD. (C) Top panel: Representative histograms of CD66b, CD15, CD16 and CD11b of LDGs and neutrophils from *P. vivax*-infected patients and neutrophils from HDs previously gated on $SSC^{hi}CD66b^{+}$. Light gray histogram: neutrophils from HDs; dark gray: LDGs; and white histogram: neutrophils from *P. vivax*-infected patients. Bottom panel: Median fluorescence intensity (MFI) scatter dot plots of the respective activation markers in LDGs (gray circles) and neutrophils (white circles) from *P. vivax*-infected patients and neutrophils from HDs (dashed line). Each circle represents one patient (n=9-16). (D) Representative zebra plot of CD34 and CD117 cell frequencies in

LDGs and neutrophils from *P. vivax*-infected patients. (A, C and D) Numbers within or beside each box refer to the cell frequencies within each gate. See also Figure S3.

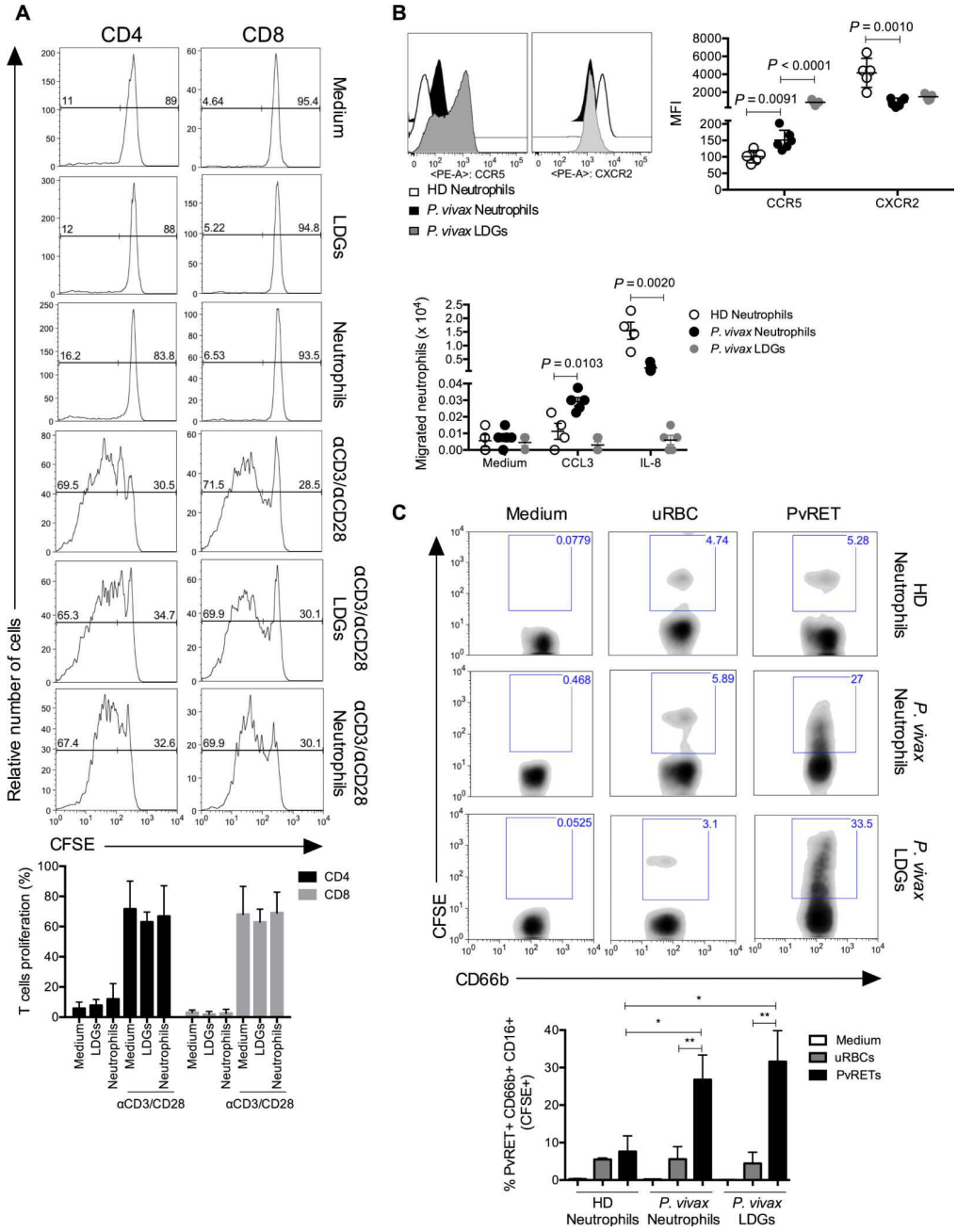

Figure 3. Functional characterization of LDGs from *P. vivax*-infected patients

(A) Top panel: CFSE-labeled PBMCs from *P. vivax*-infected patients after LDGs purification stimulated with soluble αCD3 (1 μg/mL) and αCD28 (0.5 μg/mL) in the presence or absence of LDGs or neutrophils (PBMC:LDGs or neutrophils ratio, 2:1). After four days, $CD4^+$ (left panel) and $CD8^+$ (right panel) T cell proliferation were determined by flow cytometry after gating the $CD3^+$ population and measuring the percentage of $CFSE^{low}$ T cells. Bottom panel: Percentage of CD4 and CD8 cell proliferation. Data are presented as mean ± SD (n=5). (B) Top panel: Histograms and median fluorescence intensity (MFI) of

CCR5 and CXCR2 expression in neutrophils (n=6) and LDGs (n=5) from *P. vivax*-infected patients and neutrophils from healthy donors (HD) (n=5). Bottom panel: Chemotaxis towards CCL3 (50 ng/mL) and IL-8 (10 ng/mL) evaluated in neutrophils and LDGs from *P. vivax*-infected patients (n=5) and neutrophils from HDs (n=4). Data are presented as mean ± SD. (C) Density plots (Top panel) and bar graph (bottom panel) of neutrophils (n=4) and LDGs (n=3) from *P. vivax*-infected patients and neutrophils from HDs (n=3) cocultured for one hour with purified *P. vivax*-infected reticulocytes (PvRETs) or non-infected red blood cells (uRBCs) stained with CFSE (neutrophils or LDG:PvRET or uRBCs ratio, 2:1). Numbers within each box refer to the cell frequencies within each gate. Data are represented as mean ± SEM. *0.05>P>0.01; **0.01>P>0.001.

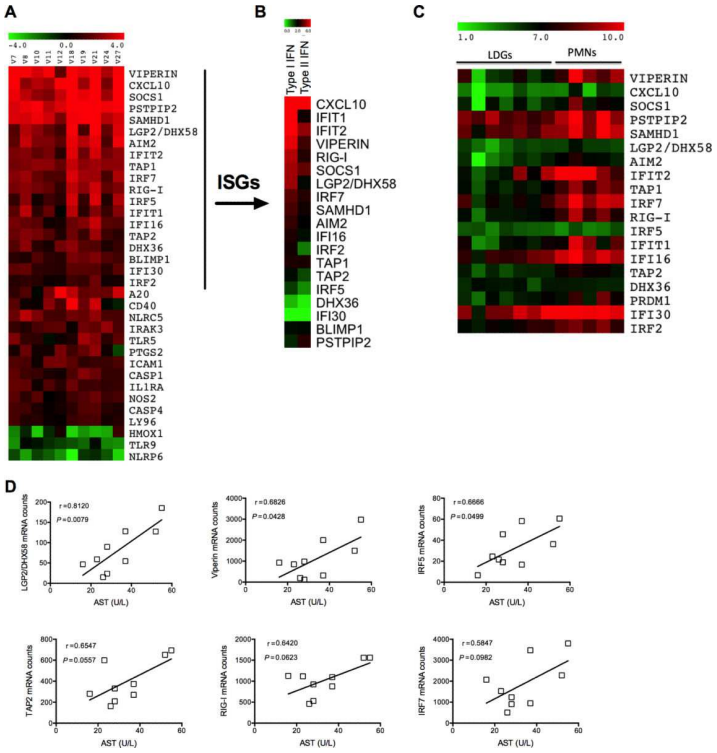

Figure 4. Neutrophils have an IFN transcriptional signature during malaria infection

(A) Nanostring analysis of purified neutrophils from 10 patients with acute *P. vivax* infections before and after Rx. Heatmap representation of 32 differentially regulated genes upon malaria infection. The heatmap shows normalized $\log_2$ ratios (*P. vivax*/after Rx) of differentially expressed genes (rows) for each patient (column). (B) Heatmap representation of a selection of ISGs that were significantly inducible during malaria infection. Neutrophils from healthy donors were stimulated with type I IFN (1000 U/mL) or IFN-γ (100 ng/mL) for 2 hours and their gene expression normalized to unstimulated cells (n=3). The heatmap shows normalized $\log_2$ ratios (Type I IFN or IFN-γ/unstimulated) of differentially expressed ISGs. (C) mRNA counts normalized to 7 housekeeping genes of LDGs (n=7) and neutrophils (n=5) from *P. vivax*-infected patients. Heatmap of ISGs that were differentially regulated upon malaria infection. (D) *LGP2/DHX58*, *VIPERIN*, *IRF5*, *TAP2*, *RIG-I* and *IRF7* mRNA counts from nanostring analysis show a trend to correlate with AST serum levels from *P. vivax*-infected patients. The results are expressed as scatter plots of individual values. Squares indicate individual patients (n=9). Pearson's rank correlation (r) and P values are shown in the graphs. See also Figure S4 and Table S1.

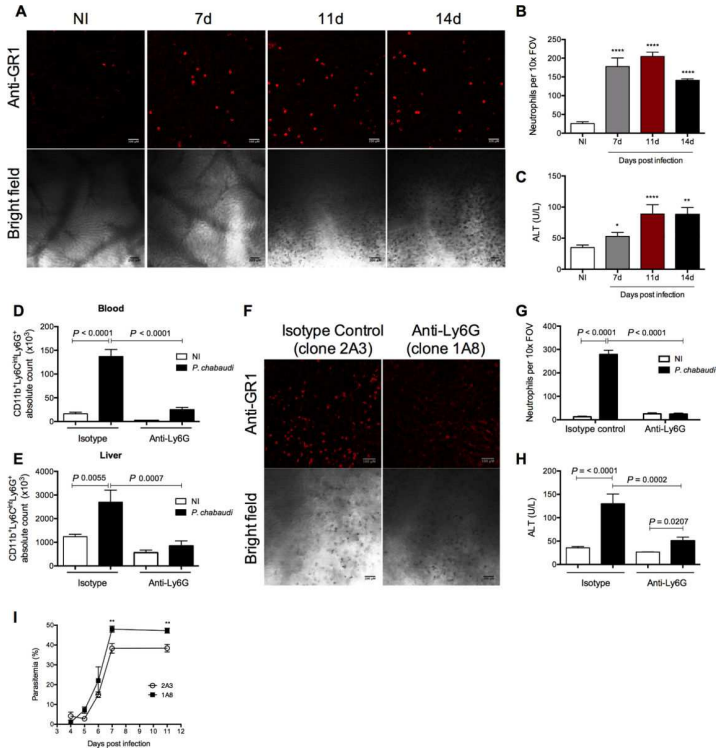

Figure 5. Following *P. chabaudi* infection neutrophils are recruited to the liver and induce liver damage

Cells were quantified by confocal intravital microscopy. (A) Representative images of bright field (bottom panel) and neutrophil staining with anti-GR1 (top panel) in liver sinusoids from non-infected (NI) and *P. chabaudi*-infected mice from different days of infection (days 7, 11 and 14). (B) Absolute numbers of GR1 positive cells from at least 4 fields of view. Results are representative of 2 independent experiments (n=4). (C) Serum ALT levels were measured at different days of *P. chabaudi* infection and in non-infected mice (n=8). The differences are relative to non-infected mice. (B and C) *0.05>P>0.01; **0.01>P>0.001;****P<0.0001. Absolute neutrophil ($CD11b^{+}Ly6C^{int}Ly6G^{+}$) quantification by flow cytometry in peripheral blood (n=8) (D) and in liver leukocytes (n=5) (E) of NI and *P. chabaudi*-infected mice treated with anti-Ly6G (clone 1A8) or with an isotype control (clone 2A3). The data are relative from 2 independent experiments. (F) Liver intravital microscopy representative images of neutrophil depletion experiment after 11 days of *P. chabaudi* infection. Cells were stained with anti-GR1 (Top panel) in mice treated or not with anti-Ly6G (clone 1A8). The bottom panel shows the bright field image of the liver. (G) Quantification of GR1 positive cells from at least 4 fields of view (n=3) and (H) serum ALT levels were measured after 11 days of infection in mice treated with anti-Ly6G (clone 1A8) or with an isotype control (clone 2A3) (n=8). (I) Parasitemia of *P. chabaudi*-infected mice treated with either anti-Ly6G or isotype control was evaluated by Giemsa staining of blood smear prepared at different days post-infection. (A and F) Scale bars: Top panel, 100 μM; bottom panel, 200 μM. (B, C, D, E, G, H and I) Data are represented as mean ± SEM. See also Figure S5 and Movie S1.

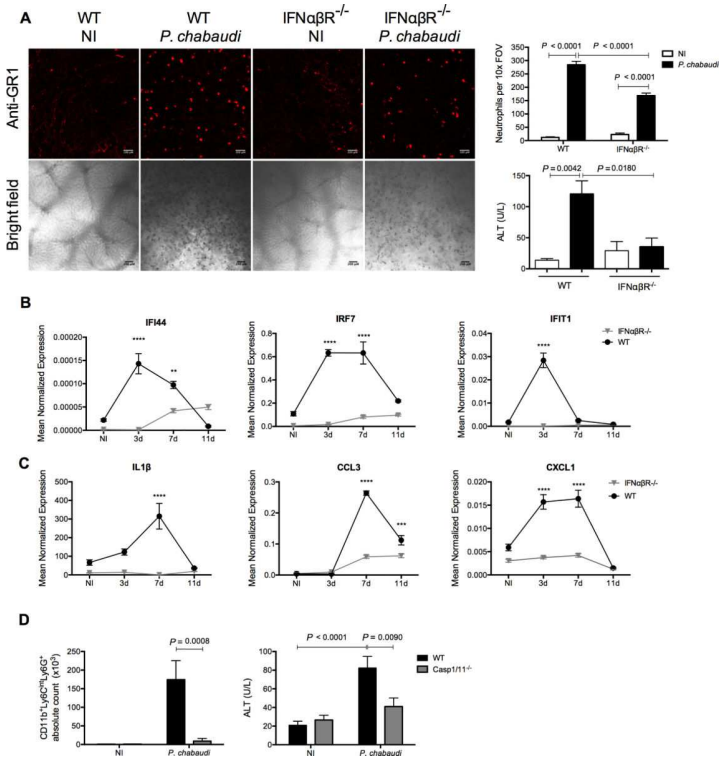

Figure 6. Type I IFN signaling and Caspase 1/11 function mediate neutrophil recruitment to the liver of *P. chabaudi* infection

(A) Intravital microscopy representative images of bright field (bottom panel) and neutrophil staining with anti-GR1 (top panel) in liver sinusoids from *P. chabaudi*-infected or non-infected WT and IFNαβR$^{-/-}$ mice. Scale bars: Top panel, 100 μM; bottom panel, 200 μM. Right panel: Quantification of GR1 positive cells from at least 4 fields of view. Results are representative of 2 independent experiments (n=4). Data are represented as mean ± SD (top). Serum ALT levels measured after *P. chabaudi* infection and in non-infected WT and IFNαβR$^{-/-}$ mice (n=4). Data are represented as mean ± SEM. mRNA expression of (B) interferon-stimulated genes *IFI44*, *IRF7* and *IFIT1* and (C) cytokines and chemokines *IL-1β*, *CCL3* and *CXCL1* in the liver of WT and IFNαβR$^{-/-}$ mice infected or not with *P. chabaudi* at different time points (3d, 7d and 11d). Data are presented as a mean ± SEM of normalized expression to the GAPDH level of 3 biological replications. The differences are relative to the WT mice. **0.01>P>0.001;***0.001>P>0.0001; ****P<0.0001. See also Table S4. (D) Absolute numbers of CD11b^{+}Ly6C^{int}Ly6G^{+} cells (left) and serum ALT levels (right) from NI and *P. chabaudi*-infected, WT and Casp1/11$^{-/-}$ mice. Data are represented as mean ± SEM (n=8). See also Figure S6.